Journal of Materials Chemistry B

Accepted Manuscript

This is an *Accepted Manuscript*, which has been through the Royal Society of Chemistry peer review process and has been accepted for publication.

Accepted Manuscripts are published online shortly after acceptance, before technical editing, formatting and proof reading. Using this free service, authors can make their results available to the community, in citable form, before we publish the edited article. We will replace this *Accepted Manuscript* with the edited and formatted *Advance Article* as soon as it is available.

You can find more information about *Accepted Manuscripts* in the Information for Authors.

Please note that technical editing may introduce minor changes to the text and/or graphics, which may alter content. The journal's standard Terms & Conditions and the Ethical guidelines still apply. In no event shall the Royal Society of Chemistry be held responsible for any errors or omissions in this *Accepted Manuscript* or any consequences arising from the use of any information it contains.

ROYAL SOCIETY OF CHEMISTRY

www.rsc.org/materialsB

Cite this: DOI: 10.1039/c0xx00000x

www.rsc.org/xxxxxx

ARTICLE TYPE

Dual endogenous stimuli-responsive polyplex micelles as smart two-step delivery nanocarriers for deep tumor tissue penetration and combating drug resistance of cisplatin

Junjie Li,[a] Yu Han,[a] Qixian Chen,*[b] Hongdong Shi,[c] Saif ur Rehman,[d] Mohammad Siddiq,[d] Yangzhong Liu,[c] Zhishen Ge*[a] and Shiyong Liu[a]

Received (in XXX, XXX) Xth XXXXXXXXX 20XX, Accepted Xth XXXXXXXXX 20XX
DOI: 10.1039/b000000x

Massive delivery of therapeutics throughout the tumor and efficient cellular internalization into tumor cells remain the major obstacles for polymeric drug delivery system in treatment of drug-resistant cancers. To address these issues, we strategically programmed dual stimuli-responsive polyplex micelles as drug delivery systems from self-assembly of anionic block copolymers, poly(ethylene glycol)-poly[(*N*′-dimethylmaleoyl-2-aminoethyl)aspartamide] (PEG-PAsp(EDA-DM)), and platinum(IV)-conjugated cationic poly(amidoamine) (PAMAM-Pt(IV)) dendrimer prodrugs. It is noteworthy that the chemical design for anionic block copolymer affords intriguing charge conversional function in response to mild acidic environment at tumor site (pH ~ 6.8), thereby permitting rapid disassembly of polyplex micelle as a result of electrostatic repulsion. Thus, PAMAM-Pt(IV) prodrugs released in the form of individual molecules exert deep penetration and well-dispersion activity in the tumor tissue by virtue of its small size and high mobility. Furthermore, the well-dispersed positively charged PAMAM dendrimers owing to its high affinity to the negatively charged cellular membrane are efficiently internalized into the tumor cells, followed by release of active cisplatin drug in the reductive cytosol. Accordingly, the drug resistance of cisplatin can be addressed. This proof-of-concept anticancer drug delivery platform provides a unique two-step delivery of anti-cancer drug for pursuit of deep tumor tissue penetration and overcoming drug resistance.

Introduction

Polymeric nanoparticles have been extensively investigated as anticancer drug delivery modality in the field of nanomedicine. As compared to conventional chemotherapy, polymeric nanocarriers have demonstrated diverse appreciable advantages.[1-5] Apparently, the targeted accumulation of anti-cancer drug will remarkably elevate drug availability to the tumor site and minimize adverse side-effect to the healthy tissues.[1,2,6] With persistent efforts for past decades, the anti-cancer drug loaded nanoparticles such as Doxil and Abraxane have gained clinical applications.[1,6] An ideal drug delivery system should protect the drug cargo sufficiently to minimize non-specific interactions with biological species and allowed efficient accumulation into the targeted sites.[7,8] Furthermore, once accumulated in tumor tissue, the drug delivery system should provide adequate penetration ability so as to deliver the drug to the entire tumor tissue for massive apoptosis of the tumor cells.[6,9-11] Nevertheless, currently clinically applicable drug delivery systems under development to date are able to afford high drug delivery efficiency to the tumor site, but failed to achieve potent tumor regression due to the lack of adequate penetration abilities.[6,12,13] Note that nanoparticles with size of ~ 100 nm are suitable for blood retention and tumor accumulation. However, the dense matrix consisting with collagen, glycosaminoglycans, and proteoglycans represents as a major barrier for deep penetration of ~ 100 nm nanoparticles inside the tumor tissue.[14-16] The attempt to overcome this barrier by releasing anti-cancer drug in the extracellular matrix (ECM) of tumor periphery can also hardly achieve deep penetration due to the existence of interstitial fluid pressure (IFP), where the drug was restricted in the perfused regions.[17] Furthermore, in regard to treatment of drug-resistant cancers, efficiently delivering drugs into entire tumor tissue and cancer cells are more essential since the tumors with multidrug resistance (MDR) will reduce cellular uptake of pure drugs or increase drug efflux.[4,18-20]

In this respect, an effective strategy to achieve tumor penetration is to create stimuli-responsive size-alterable nanoparticles which are functionalized with controllable structural rearrangement to satisfy the requirements of the deep tumor tissue penetration.[21,22] Pioneer researches have demonstrated the feasibility of chemistry based strategy to obtain such functionalities. As a typical example, Fukumura et al.[22] reported a quantum dots-encapsulated gelatin nanoparticle with shrinkable size triggered by proteases that are highly expressed in the tumor microenvironment such as matrix metalloproteinase-2 (MMP-2). The MMP-2 could degrade the cores of 100-nm gelatin

Journal of Materials Chemistry B Accepted Manuscript

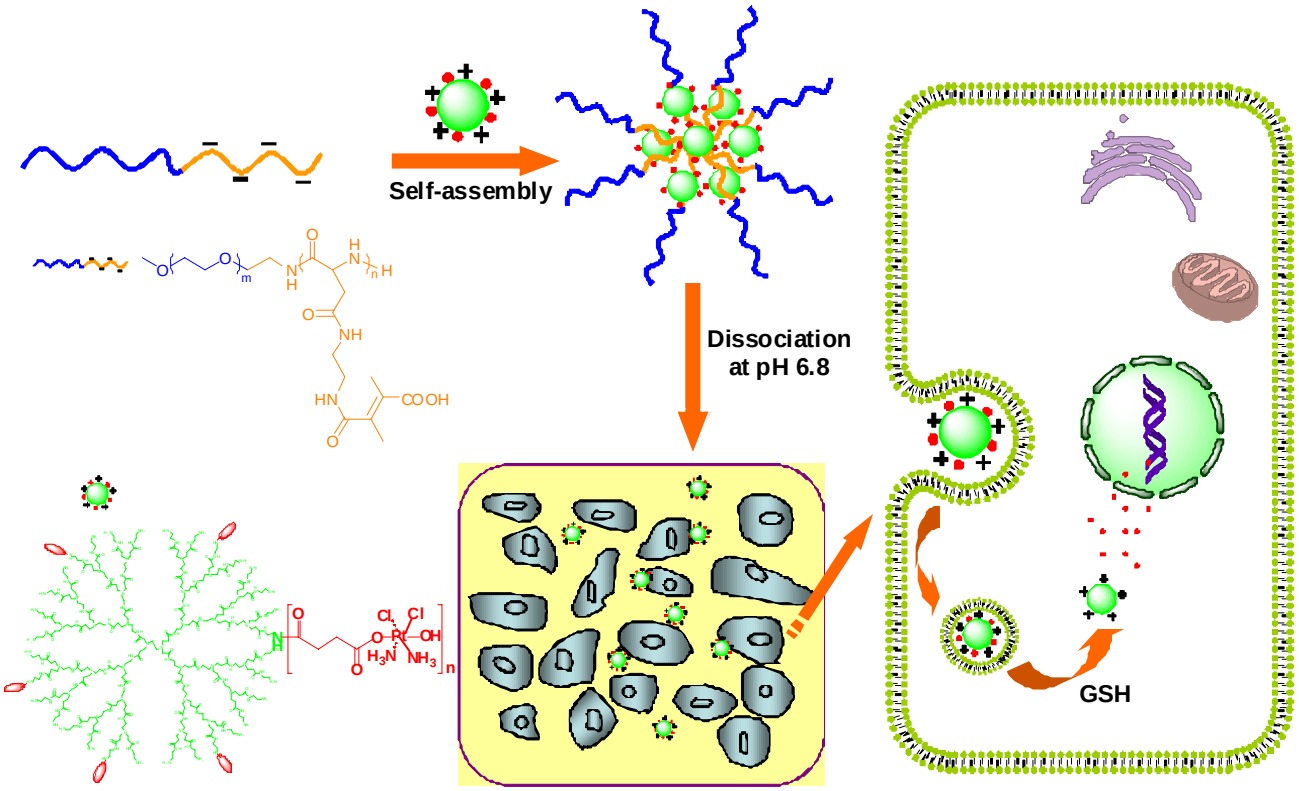

Scheme 1 Schematic illustration of polyplex micelles in response to mildly acidic and reductive environment exhibiting two-step delivery for deep tumor tissue penetration and intracellular cisplatin release.

nanoparticles, releasing smaller 10-nm quantum dots (QD) nanoparticles from their surface. On the other hand, the size alterable nanoparticles were designed in response to the external stimuli (e.g. light) by Kohane et al.[21] They designed a nanoparticulate drug delivery system that underwent reversible volume transition from 150 to 40 nm upon phototriggering with UV light. These monodispersed nanoparticles consisting of spiropyran, which underwent reversible photoisomerization, and PEGylated lipid enabled repetitive dosing, accordingly sufficing for enhanced tissue penetration. However, taken into account the practical clinical operation, more biocompatible nanoparticles and practicable stimuli methods are imperative to be further explored.

As aforementioned, to overcome the issue of deep tumor tissue penetration, the multi-stage delivery systems responsive to tumor tissue or intracellular microenvironments should be effective strategies.[22-24] As a proof of concept addressing this issue, we programmed a polyplex micelle delivery system from complexation of *c,c,t*-[$Pt(NH_3)_2Cl_2(OH)(O_2CCH_2CH_2CO_2H)$]-conjugated cationic poly(amidoamine) (PAMAM-Pt(IV)) prodrugs and anionic block copolymers consisting of biocompatible poly(ethylene glycol) (PEG) segment and anionic segment with appreciable tumor tissue acidity-responsive charge conversional function. The constructed drug delivery system provides distinct two-step delivery kinetics under the stimuli of tumor environment and intracellular microenvironments. At tumoral acidic pH, the polyplex micelles can easily disassemble due to charge conversion reaction of anionic polymer, in consequence releasing molecular PAMAM-Pt(IV) prodrugs, which anticipate for deep tissue penetration. Furthermore, the positively charged PAMAM-Pt(IV) prodrugs endows high affinity with anionic cell surface, accordingly eliciting high cellular uptake. Ultimately, active anticancer drug cisplatin can be released under the reductive environment inside the cells, which thus provides a convenient way to overcome the drug resistance for intracellular delivery to the tumor cells (Scheme 1). In this work, deep tissue penetration and high cellular uptake as a consequence of polymer micelle dissociation at mild acidic environment, as well as drug release in reductive cytosol were demonstrated. Moreover, the behaviors of deep tissue penetration and the efficiency for overcoming drug resistance of cisplatin were examined using collagen gel diffusion, multicellular tumor spheroids (MCTS) from cisplatin resistant cancer cell lines A549R.

Experimental section

Materials

The third and fourth generation poly(amidoamine) (G3-PAMAM and G4-PAMPAM) dendrimers were purchased from Weihai CY Dendrimers Technology Co., Ltd. (Shandong, China). Rat tail tendon collagen type I was obtained from Shanghai Canspec Scientific Instruments Co., Ltd. (Shanghai, China). 1-(3-Dimethylaminopropyl)-3-ethylcarbodiimide hydrochloride (EDC, 98%), *N*-hydroxysuccinimide (NHS, ≥98%), Fluorescein isothiocyanate (FITC), Succinic anhydride, and 2,3-dimethylmaleic anhydride were obtained from Sigma-Aldrich and used as received. *N*,*N*-dimethylformamide (DMF), dichloromethane (CH_2Cl_2), *N*-methyl-2-pyrrolidone (NMP), and ethylenediamine (EDA) were dried over CaH_2 and distilled

Journal of Materials Chemistry B Accepted Manuscript

before use. α-Methoxy-ω-amino-poly(ethylene glycol) (PEG-NH_2, M_w = 12,000 and 20,000) was obtained from Nippon Oil and Fats Co., Ltd. (Tokyo, Japan). β-Benzyl-L-aspartate *N*-carboxyanhydride (BLA-NCA) was obtained from Chengdu Enlai Biological Technology Co., Ltd. (Chengdu, China). Block copolymers, PEG-poly[(2-aminoethyl)aspartamide] (PEG_{454}-$PAspEDA_{96}$ (M_n = 41,300 M_w/M_n = 1.11) and PEG_{273}-$PAspEDA_{68}$ (M_n = 24,700 M_w/M_n = 1.10)), were synthesized according to method provided in the literature.[25] Cisplatin was purchased from Shandong Boyuan Pharmaceutical Co., Ltd. (Shandong, China). The Pt(IV) prodrug, *c,c,t*-$[Pt(NH_3)_2Cl_2(OH)(O_2CCH_2CH_2CO_2H)]$, was synthesized from cisplatin according to established procedures provided in the literature.[26] Fetal bovine serum (FBS), trypsin, Dulbecco's modified Eagle's medium (DMEM), and RPMI-1640 medium were purchased from GIBCO and used as received. Cell culture lysis buffer, 4',6-diamidino-2-phenylindole (DAPI), Lyso-Tracker Red, 3-(4,5-dimethylthiazol-2,5-diphenyltetrazolium bromide (MTT), and Enhanced BCA Protein Assay Kit were purchased from Beyotime Institute of Biotechnology. The human lung cancer cell line A549 and cisplatin resistant human lung cancer cell line A549R were purchased from Cell Bank of Chinese Academy of Sciences (Shanghai, China) and Shanghai Fumengjiyin biotechnology Co. Ltd., respectively. All other commercially available solvents and reagents were purchased from Sinopharm Chemical Reagent Co. Ltd. and used as received.

Sample preparation

The synthetic procedures for PEG-poly[(*N*′-dimethylmaleoyl-2-aminoethyl)aspartamide] (PEG-PAsp(EDA-DM)) and PEG-poly[(*N*′-succinyl-2-aminoethyl)aspartamide] (PEG-PAsp(EDA-SU) block copolymers, PAMAM-Pt(IV) and PAMAM-FITC dendrimers are shown in Scheme S1.

The brief procedures to amidize the block copolymer with anhydrides was described as follows. PEG_{454}-$PAspEDA_{96}$ (0.1 g, 0.28 mmol amino groups) was dissolved in 2 mL of deionized water and pH of the solution was adjusted to be 8.5. Upon addition of 2,3-dimethylmaleic anhydride (0.36 g, 2.86 mmol), the solution pH value was maintained at 8.5 with NaOH. The reaction was carried out at room temperature for 90 min. The solution was dialyzed against distilled water for three times at pH 8.5. The final solution was lyophilized to yield PEG_{454}-$PAsp(EDA\text{-}DM)_{96}$ block polymer as the sodium salt form (0.13 g, 91.6%). ^{1}H NMR measurement was conducted to give quantitative estimation of transformation of amino groups into carboxyl moieties. The other block copolymers, PEG_{454}-$PAsp(EDA\text{-}SU)_{96}$, PEG_{273}-$PAsp(EDA\text{-}DM)_{68}$, and PEG_{273}-$PAsp(EDA\text{-}SU)_{68}$, were synthesized according to a similar procedure.

PAMAM-Pt(IV) prodrug was synthesized according to a EDC/NHS coupling method. Powder of EDC (0.19 g, 1 mmol) and NHS (0.12 g, 1 mmol) were sequentially dissolved in 4 ml DMSO under stirring, followed by addition of *c,c,t*-$[Pt(NH_3)_2Cl_2(OH)(O_2CCH_2CH_2CO_2H)]$ (0.2 g, 4.61×10^{-4} mol). After stirring for 30 min, G3-PAMAM (0.4 g, 5.76×10^{-5} mol) in 2 ml DMSO was added for reaction at room temperature for 24 h. Then reaction mixture was dialyzed against distilled water for 12 h and lyophilized to yield PAMAM-Pt(IV) prodrug. The Pt content in PAMAM was quantified by platinum ICP-MS measurement, and the number of Pt(IV) per G3-PAMAM dendrimer was estimated to be 5. G4-PAMAM-Pt(IV) was prepared with 12 Pt(IV) per G4-PAMAM dendrimer according to a similar procedure.

FITC was attempted to be coupled with PAMAM by the reaction between isothiocyanate and amino groups. In brief, G3-PAMAM (0.2 g, 2.90×10^{-5} mol) was dissolved in methanol, followed by addition of FITC (67.8 mg, 1.74×10^{-4} mmol). After stirring at room temperature for 24 h, the reaction solution was dialyzed against distilled water for 48 h and lyophilized to yield PAMAM-FITC conjugates. According to ^{1}H NMR measurement of product in DMSO-d_6, the number of fluorescein molecules conjugated to PAMAM was determined to be 4.

Preparation of the polyplex micelles

Block copolymers, PEG-PAsp(EDA-DM) or PEG-PAsp(EDA-SU), and PAMAM-Pt(IV) or PAMAM-FITC were separately dissolved in 10 mM PBS buffer (pH 7.4) as stock solutions. The polyplex micelles were formed by addition of dendrimer solution into block copolymer solution for complexation at charge ratio of 1, followed by incubation 0.5 h at 4 ^{o}C. The formed polyplex micelles, PEG_{454}-$PAsp(EDA\text{-}DM)_{96}$/G3-PAMAM-Pt(IV), PEG_{454}-$PAsp(EDA\text{-}SU)_{96}$/G3-PAMAM-Pt(IV), PEG_{454}-$PAsp(EDA\text{-}DM)_{96}$/G3-PAMAM-FITC, and PEG_{454}-$PAsp(EDA\text{-}SU)_{96}$/G3-PAMAM-FITC were denoted as **PM1**, **PM2**, **PM3**, and **PM4**, respectively.

Dynamic light scattering (DLS) measurement

The time-dependent particles size, light scattering intensity, and ξ-potential of polyplex micelles were monitored by the dynamic light scattering technique (DLS) using a Zetasizer Nano ZS. The polyplex micelles, **PM1** and **PM2** were separately incubated in 10 mM PBS buffer at pH 7.4 and 37 ^{o}C. After 10 h incubation, the solution pH was adjusted to 6.8. The time-dependent particles size, light scattering intensity, and ξ-potential of PIC micelles were recorded when equilibrium reached.

Drug release from the polyplex micelles PEG-PAsp(EDA-DM)/PAMAM-Pt(IV)

In vitro release of cisplatin drug from polyplex micelles PEG-PAsp(EDA-DM)/PAMAM-Pt(IV) under diverse conditions was studied using a dialysis bag diffusion method. In brief, 10 mg of **PM1** in 2 mL 10 mM PBS (pH 7.4) was injected into a pre-swelled dialysis bag with a molecular weight cutoff of 3.5 kDa, followed by immersion into 18 ml of 10 mM PBS (pH 7.4). The dialysis was conducted at 37°C in a shaking culture incubator. Periodically, 1 mL aliquot of sample solution from the incubation medium was taken for measurement and compensated with 1 mL of fresh buffer to incubation medium. The concentration of platinum in the released solutions was quantified by ICP-MS measurement. The platinum released from the micelles was expressed as the percentage of cumulative platinum outside the dialysis bag to the total platinum in the micelles. The same drug release procedure was also applied for the quantification of release profile of polyplex micelles at pH 7.4 in the presence of 10 mM DTT or at pH 6.8 in the presence and absence of 10 mM DTT.

Cellular viability cultured at pH 6.8

Journal of Materials Chemistry B Accepted Manuscript

A549 and A549R cells were seeded onto 96-well plates, respectively, at a density of 1×10^4 cells/well in 200 μL DMEM with 10% FBS at 37 °C with 5% CO_2 humidified atmosphere. After incubation overnight, the original medium was replaced with fresh medium of pH 6.8. After incubation for a predetermined time, MTT solution (20 μL, 5 mg/mL in PBS buffer) was added to each well, followed by 4 h incubation. The medium in each well was then removed and 200 μL of DMSO was added to dissolve the internalized purple formazan crystals. The plate was gently agitated for 2 h until all the crystals were dissolved. The absorbance at 490 nm was recorded by a microplate reader (Thermo Fisher). The time-dependent relative cell viability cultured at pH 6.8 was presented by comparing with that cultured at pH 7.4.

In vitro cytotoxicity evaluation

A549 and A549R cells were used for *in vitro* cytotoxicity evaluation of polyplex micelles based on a MTT assay. A549 cells were seeded onto 96-well plates at a density of 1×10^4 cells/well in 200 μL DMEM with 10% FBS at 37°C with 5% CO_2 humidified atmosphere. A549R cells were seeded onto 96-well plates at a density of 1×10^4 cells/well in 200 μL RPMI-1640 medium with 10% FBS at 37 °C with 5% CO_2 humidified atmosphere. After 24 h incubation, the original medium was replaced with pH 7.4 or 6.8 culture medium, followed by addition of cisplatin, **PM1**, or **PM2** in a concentration-dependent manner, respectively. After 3 h incubation, the medium in each well was replaced with fresh cell culture medium for another 48 h incubation. MTT solution (20 μL, 5 mg/mL in PBS buffer) was added to each well and incubated 4 h for reaction. The medium in each well was then removed and 200 μL of DMSO was added to dissolve the internalized purple formazan crystals. The plate was subjected to gently agitation for 15 min until all the crystals were dissolved. The absorbance at wavelength of 490 nm was recorded by a microplate reader (Thermo Fisher).

In order to conduct viability staining, A549R cells were seeded onto 6-well plates at a density of 1×10^5 cells/well in 2 mL RPMI1640 medium with 10% FBS at 37°C with 5% CO_2 humidified atmosphere followed by incubation overnight for cell attachment. The medium was removed, followed by addition of 2 mL **PM1** or **PM2** containing culture medium of pH 7.4 or pH 6.8 at an entire Pt(IV) concentration of 0.6 μM. After 3 h incubation, the medium in each well was replaced with fresh cell culture medium followed by another 24 h incubation. Then, medium was replaced with 2 mL PBS solution. Each well was treated with 8 μL calcein AM stock solution (1 mg/mL in DMSO) followed by 30 min incubation at ambient temperatures. Subsequently, PBS was removed and 2 mL propidium iodide (PI) solution (50% in PBS) was added to each well followed by 5 min incubation. After that, each well was rinsed twice with 3 mL of PBS. Finally, cells immersed in 4 mL of PBS were taken for fluorescence imaging by using a confocal laser scanning microscopy (CLSM) (Leica TCS SP5, Germany).

Cellular internalization and intracellular distribution of the polyplex micelles using CLSM

Cellular internalization and intracellular distribution of the polyplex micelles against A549R cells were observed using CLSM. A549R cells were seeded at a density of 1×10^4 cells/well into a 35-mm glass-bottom culture dish (NEST, China) and cultured overnight in 2 mL RPMI-1640 medium with 10% FBS at 37 °C with 5% CO_2 humidified atmosphere. The medium was removed, followed by addition of 2 mL **PM3** or **PM4** containing 2 mL culture medium of pH 7.4 or pH 6.8 at an equivalent FITC concentration of 1 mM. After 3 h incubation, cells were washed three times with ice-cold PBS. Cell nuclei and lysosome were counterstained with DAPI (Blue) and Lyso-Tracker (Red), respectively. Then, cells were washed three times with ice-cold PBS and observed under CLSM.

Cellular uptake measured by flow cytometry and ICP-MS

The cellular uptake efficiency of the polyplex micelles in A549R cells was determined by flow cytometry and ICP-MS, respectively. In brief, A549R cells were seeded in 6-well plates at a density of 1×10^5 cells/well in 2 mL RPMI-1640 medium with 10% FBS at 37°C with 5% CO_2 humidified atmosphere and incubate overnight for cell attachment onto the substrate. The medium was removed, followed by addition of 2 mL **PM3** or **PM4** containing culture medium of pH 7.4 or pH 6.8 at an entire FITC concentration of 1 mM. After 3 h incubation, the cells were washed three times with PBS to remove extracellular polyplex micelles. After detachment by trypsin treatment from the culture plate, the cells were harvested and resuspended in PBS for flow cytometry measurement. Data were analyzed with Flowjo software.

On the other hand, A549R cells were seeded in 6-well plates at a density of 1×10^5 cells/well in 2 mL RPMI-1640 medium with 10% FBS at 37 °C with 5% CO_2 humidified atmosphere and incubate overnight for cell attachment onto the substrate. The medium was removed, followed by addition of 2 mL **PM1** or **PM2** containing culture medium of pH 7.4 or pH 6.8 at an entire Pt(IV) concentration of 0.4 μM. After 3 h incubation, the cells were washed three times with ice-cold PBS and lysed in 500 μL of the cell culture lysis buffer. Aliquots were removed and the total amount of cellular protein was determined by a BCA Protein Assay. The Pt content in cells was determined by ICP-MS measurement. The final results were expressed as ng Pt/mg protein. The cellular uptake of anticancer drug cisplatin was also evaluated according to a similar procedure.

Collagen gel diffusion

Collagen hydrogels were prepared according the manufacture's protocol by mixing 50 μL of 8 mg/mL rat tail collagen I and 3 μL of 0.1 M sodium hydroxide on ice. The final concentration of collagen was 7.54 mg/mL. After vortexing, the gel was added to partially fill a microslide capillary tube followed by overnight incubation at 37°C. 20 μL of **PM3** at an entire FITC concentration of 1 mM were incubated at pH 7.4 or pH 6.8 for 1 h, followed by addition of 3μL micelle solutions into the capillary tube to ensure contact with the surface of the collagen gel. The sample was incubated for diffusion at 37°C for 4 h and then imaged using CLSM.

Penetration and growth inhibition study in A549R multicellular tumor spheroids (MCTS)

In order to produce A549R MCTS, a layer of poly(2-hydroxyethyl methacrylate) (PHEMA) thin film was coated on the bottom of tissue culture flasks.[27] Then, PHEMA coated flask

Journal of Materials Chemistry B Accepted Manuscript

was exposed to ultraviolet light for 2 h to ensure sterile before use. A single-cell suspension of 5×10^5 A549R cells in 5 mL of fresh RPMI-1640 medium with 10 % FBS was incubated in a cell culture flask coated by PHEMA at 37°C in humidified atmosphere with 5% CO_2. The culture medium was replaced with fresh one every other day. A549R MCTS with diameter of ~ 300 μm were formed spontaneously in 7 days.

A549R MCTS with the diameter of ~ 300 μm were harvested at day 7. For each experiment, ~ 20 spheroids were handpicked with a Pasteur pipette and transferred to a 35-mm glass-bottom culture dish coated with PHEMA in 2 mL RPMI-1640 with 10% FBS at 37°C with 5% CO_2 humidified atmosphere. **PM3** were added to the suspension of spheroids at an entire FITC concentration of 1 mM, waiting for desired time under incubation at pH 7.4 or 6.8. The medium was then removed and MCTS were washed with PBS prior to CLSM observation. The semi-quantitative analysis of mean fluorescence intensity of FITC in MCTS was conducted by CLSM.

The inhibitory effect of **PM1** at pH 6.8 and 7.4 to MCTS were evaluated. The A549R MCTS with the diameter of ~ 300 μm were harvested at day 7. Then, ~ 20 spheroids were handpicked with a Pasteur pipette and transferred to a 35-mm glass-bottom culture dish coated with PHEMA in 2 mL RPMI-1640 with 10% FBS at 37°C with 5% CO_2 humidified atmosphere. **PM1** were added to the suspension of spheroids at an entire Pt concentration of 0.4 μM, and incubated at pH 7.4 or 6.8 for 24 h, then incubated with fresh culture medium for another 6 days and the culture medium was refreshed every day. The diameters of spheroids were measured from images taken by optical microscopy.

Characterization

All nuclear magnetic resonance (NMR) spectra were recorded on a Bruker AV300 NMR 300 MHz spectrometer using DMSO-d_6 or D_2O as the solvent. Molecular weights and molecular weight distributions were determined by gel permeation chromatography (GPC) equipped with an Agilent 1260 pump and an Agilent G1362A differential refractiveindex detector. The eluent was ultrapure water with 50 mM NaCl and 10 mM acetic acid at a flow rate of 1.0 mL/min. A series of low polydispersity PEG standards were employed for calibration. ξ-potentials, particles sizes, and particle size distributions were conducted on a ξ-potential analyzer with dynamic laser light scattering (DLS), equipped a Malvern Zetasizer Nano ZS90, a He-Ne laser (633 nm), and 90^o detector optics. All data were averaged over three measurements. All samples were filtered through 0.45 μm Millipore Acrodisc-12 filters to remove dust prior to use. Transmission electron microscopy (TEM) observations were conducted on a Hitachi H-800 electron microscope at an acceleration voltage of 200 kV. Platinum content was measured on an X Series 2 Inductively Coupled Plasma Mass Spectrometer (ICP-MS, Thermo fisher Scientific). Flow cytometric analysis was conducted using a BD FACSCalibur flow cytometer with the excitation wavelength set to be 488 nm.

Results and discussion

Sample preparation and formation of polyplex micelles

The pH-responsive charge-conversional block polymers were prepared by introduction of citraconic amide to the side chain of the block copolymers in the previous report. Pioneer researches have claimed the charge conversion in acidic endosomal milieu in term of cleavage of amide bond.[25,28] Then, a series of the amide formulations was encouraged to be synthesized from varying anhydrides, and the degradation efficiency can be examined by adjusting incubation pH values.[29] Interestingly, the amide prepared from 2,3-dimethylmaleic anhydride was distinguished to be cleavable at tumor tissue weakly acidic microenvironment (~ pH 6.8).[29-31] Thus, this amide was chosen to prepare the negatively charged segments in the block copolymers. The precursor block copolymer, PEG-PAsp(EDA), was synthesized as previously reported.[25] The amidized final products, PEG-PAsp(EDA-DM) and PEG-PAsp(EDA-SU), were synthesized via an amidization reaction with anhydride in aqueous solution at pH 8.5 (Scheme S1A). To verify the pH-induced charge conversion of block copolymer under mild acidic conditions, PEG-PAsp(EDA-DM), ^{1}H NMR measurements were carried out to evaluate the cleavage degree of amide groups. The signal of the proton resonance of two methylene groups adjacent to amide groups (a + b) is supposed to shift toward higher (c) and lower fields (d), respectively, upon cleavage of amide groups. The relative intensity of the signals from CH2-amide and CH2-amine proved that more than 80% amide groups were hydrolyzed for 1 h at pH 6.8 (Fig. S1). In contrast, the block copolymer, PEG-PAsp(EDA-DM), is relatively stable at pH 7.4 as evidenced by less than 20% amide hydrolysis after 10 h incubation (data not shown). On the other hand, the control block copolymers, PEG-PAsp(EDA-SU) without cleavage function, preserved chemical structural integrity at pH 7.4 and 6.8 owing to high stability of the amide.

PAMAM dendrimers were recognized as promising candidates for the preparation of polymeric nanoparticles in the field of nanomedicine, which are expected to provide diverse advantageous features including monodisperse, nanoscale sizes, mathematically defined numbers of terminal surface groups suitable for bioconjugation of bio-active molecules such as drugs or imaging agents, tunable surfaces for enhanced cellular uptake, choice of low generation for biocompatibility [e. g. G = 1-5 for PAMAM dendrimers].[32-36] On the other hand, the small size and tunable surface characters are especially beneficial for penetration inside tissues given that small and positively charged nanoparticles have been demonstrated to improve delivery of payloads to the majority of cells in tumors by virtue of deep tissue penetration and high uptake traits.[37-40] In this study, PAMAM-Pt(IV) prodrugs were synthesized from PAMAM and *c*,*c*,*t*-[$Pt(NH_3)_2Cl_2(OOCCH_2CH_2COOH)(OH)$] using EDC/NHS coupling reaction in DMSO (Scheme S1b). In order to preserve the positive charges for polyion complexation and cellular uptake use, merely ~ 10 % of the amine groups were utilized for Pt(IV) conjugation on the surface of dendrimer, and subsequent ICP-MS measurements confirmed that 12 units per G4-PAMAM and 5 units per G3-PAMAM, respectively. Notably, upon direct dissolution of dendrimers into aqueous solution at pH 7.4, dendrimers with ~ 10% Pt(IV) conjugate allowed for molecular dispersion as supported by several nm of $<D_h>$ from DLS measurements. To trace the dendrimers, FITC molecules were also conjugated onto the surface of dendrimer with a similar conjugation ratio.

Journal of Materials Chemistry B Accepted Manuscript

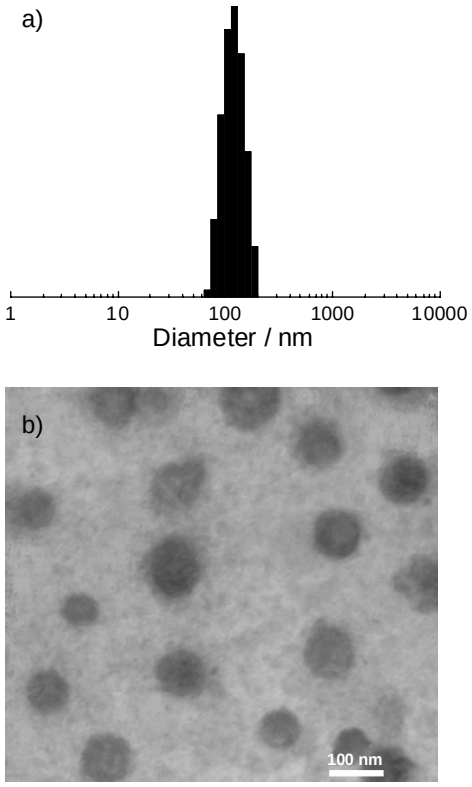

Fig. 1 Characterization of **PM1** with the total concentration of 1 mg/mL in aqueous solution at 10 mM PBS buffer (pH 7.4). (a) Size measurements and (b) TEM morphologies of **PM1**.

Considering that the surface amine groups of PAMAM dendrimers with pK_a values ~ 10.0 are protonated at physiological pH, thus, they behave as positively charged residues for electrostatic assembly with negatively charged molecules. On the other hand, tertiary amine groups in the interior pockets of PAMAM dendrimers possessing pK_a values ~ 6.0 endow favorable pH buffering capability, accordingly able to facilitate endosomal escape of the PAMAM-based nanoparticles.[41] The polyplex micelles between negatively charged block copolymers and positively charged PAMAM dendrimer conjugated by Pt(IV) were obtained by mixing their aqueous solutions at pH 7.4 buffer with the stoichiometric charge ratio. In this study, four groups of polyplex micelles were prepared from the block copolymers, PEG_{273}-PAsp(EDA-DM)$_{68}$ or PEG_{454}-PAsp(EDA-DM)$_{96}$, and G3 or G4-PAMAM-Pt(IV) dendrimers at the total polymer concentration of 1 mg/mL. As shown in Table S1, DLS characterization revealed that the polyplex micelles (**PM1**) from PEG_{454}-PAsp(EDA-DM)$_{96}$ and G3-PAMAM-Pt(IV) dendrimer exhibited as the most appreciable candidate in respect to its most uniform size with lowest size distribution μ_2/Γ^2 of 0.091 and relatively small size with $\langle D_h \rangle$ of 142.3 nm (Fig. 1a). Thus, **PM1** were chosen as optimized system for the hereafter evaluation. For comparison, polyplex micelles (**PM2)** from PEG_{454}-PAsp(EDA-SU)$_{96}$ without charge conversion function and G3-PAMAM-Pt(IV) was also prepared, which exhibited similar μ_2/Γ^2 of 0.1 and $\langle D_h \rangle$ of 150.7 nm. Furthermore, TEM image showed that **PM1** with distinct spherical shape (Fig. 1b). The particle sizes in TEM images selectively reflected the polyplex cores due to high contrast of PAMAM-Pt(IV) prodrug, whereas the hydrophilic shell of the polyplex micelles were not observed due to low contrast in TEM images.

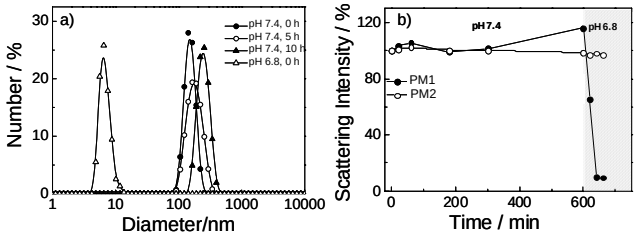

Fig. 2 The structural stability of polyplex micelles with incubation at pH 7.4 or 6.8. (a) Size distribution of **PM1** after incubation for a desired time. (b) Time-dependent light scattering intensity of **PM1** and **PM2** at pH 7.4 or pH 6.8.

Tumoral acidity-responsive property of the polyplex micelles

As the amide bond cleaved to restore amine groups under mild acidic pH, negatively charged PEG-PAsp(EDA-DM) block copolymer gradually transformed to positively charged PEG-PAspEDA. This charge conversion reaction will generate strong repulsion force to cationic G3-PAMAM-Pt(IV) component, eventually leading to the polyplex micelle falling apart.[25,28] Subsequently, the ξ-potential of the nanoparticles should convert from neutral to positive with the charge conversion reaction of the block copolymers. Simultaneously, the particle size and light scattering intensity of the polyplex micelles should undergo distinct drop due to disassembly of the polyplex micelles. To verify this hypothesis, **PM2** was used as a control to investigate the effect of charge conversion on the structure of polyplex micelle. Two types of polyplex micelles, **PM1** and **PM2**, were initially incubated in aqueous solution at pH 7.4. The ξ-potential and DLS measurements showed that the polyplex micelles, **PM2**, remained stable with incubation time up to 11 h as evidenced by the constant ξ-potentials and light scattering intensity despite of adjusting pH values from 7.4 to 6.8 (Fig. 2b and S2). On the other hand, as for **PM1**, ξ-potential and light scattering intensity increased slightly within 10 h incubation at pH 7.4 with the particle sizes increasing from 142.3 nm to 209.8 nm, probably since slow amide cleavage reaction existed at pH 7.4. In stark contrast, **PM1** underwent dramatic change in both of ξ-potential and DLS measurement as the incubation pH was adjusted from 7.4 to 6.8. The ξ-potential increased from almost neutral to ~ 5 mV, and the light scattering intensity dropped dramatically within 1 h in company with size transition from 209.8 nm to several nm, suggesting the dissociation of the polyplex micelles and release of G3-PAMAM-Pt(IV) prodrugs (Fig. 2 and S2). These results approved the strategic design for polyplex micelles with charge conversion function for release of drug conjugates under tumor acidic microenvironment while keeping relatively stable at neutral pH.

Drug release from polyplex micelles

Pt(IV) prodrug was reported to be converted into active cisplatin in the intracellular reductive environment. Under a reductive condition, cisplatin was demonstrated to be the predominant product since the hydrolysis of ester bonds linker of the Pt(IV) prodrug are relatively slow as compared to transformation from Pt(IV) to cisplatin (II).[42] Therefore, a variety of delivery systems

Journal of Materials Chemistry B Accepted Manuscript

were encouraged to utilize Pt(IV) prodrugs as therapeutic cargo.[20,42-45] To quantify the intracellular released cisplatin, we performed the release experiments based a dialysis method against saline buffer with a 3.5 kDa molecular weight cutoff membrane under diverse incubation conditions including pH 7.4 or pH 6.8, in the presence or absence of DTT, respectively. The released platinum was quantified by ICP-MS measurement. As shown in Fig. 3, markedly rapid release of platinum was observed for the sample by treatment of reductive agent DTT as compared to those in absence of DTT. In absence of DTT only ~ 15% of Pt was released for the sample with 14 h incubation at pH 7.4 and pH 6.8, indicating that the first stage delivery vehicle (polyplex micelles) and second stage delivery carrier (PAMAM) can protect Pt(IV) from transformation before cellular internalization. However, more than 50% of Pt was released just after initial 3 h incubation in presence of 10 mM DTT and as high as 80% of Pt was released after 14 h at both pH of 7.4 and 6.8, suggesting that both prodrugs loaded in polyplex micelles can be effectively transformed into active cisplatin form inside the cells.

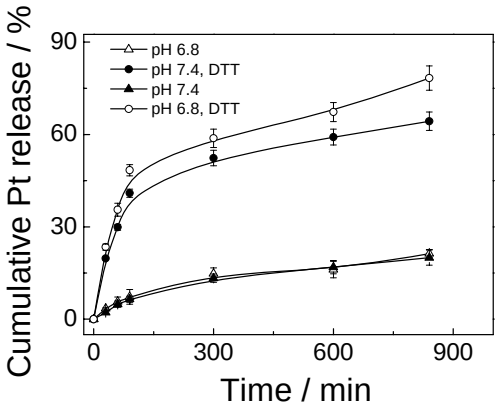

Fig. 3 Drug release profiles of **PM1** at pH 7.4 or pH 6.8 in the presence or absence of 10 mM DTT (mean ± SEM, n =3).

Cellular uptake

We firstly evaluated the cell viability cultured under mildly acidic condition (pH 6.8) (Fig. S3). The results showed that this very slight pH variation did not affect the cell viability obviously within 48 h. Cellular uptake efficiency of polyplex micelles in cisplatin-resistant cancer cells A549R was then evaluated by observation and quantification of fluorescence intensity given by FITC. PAMAM dendrimer was labeled with FITC (PAMAM-FITC) was used to prepare polyplex, and the polyplex micelles formulated from PEG-PAsp(EDA-DM) block copolymers and PAMAM-FITC possessing similar physical characters (size and size distribution) to those prepared from Pt(IV)-conjugated dendrimers. Prior to applying polyplex micelles into the cells, A549R cells were incubated at pH 7.4 or pH 6.8, respectively. Then, **PM3** or **PM4** with the equal amount of FITC was added into A549R cells, followed by 3 h incubation. The fluorescence cell images were captured after thorough washing to remove extracellular nanoparticles. As shown in Fig. 4a, the strong intracellular fluorescence (green) was only observed for **PM3** at pH 6.8. A plausible reason for this is that the pH-responsive charge conversion of polyplex micelle at pH 6.8 induced micellar dissociation and release of positively charged PAMAM dendrimers thus readily uptake by the cells. In the previous reports, PAMAM dendrimers of third or higher generation demonstrated to promote cellular uptake remarkably via high affinity with cell membrane.[46,47] In contrast, the polyplex micelles with entire structural integrity can hardly be internalized by the cells due to PEG passivation with cellular membrane.[48-50] Furthermore, the cellular uptake of the polyplex micelles was evaluated quantitatively by flow cytometry. In consistency, only **PM3** at pH 6.8 presented markedly high cellular uptake activity (Fig. 4b and c).

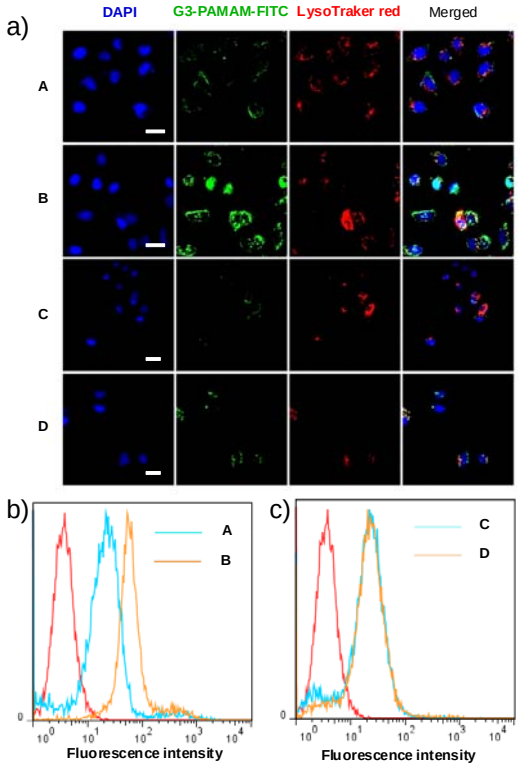

Fig. 4 (a) CLSM observation of the intracellular distribution of polyplex micelles with late endosomes/lysosomes (red) and nuclei (blue) in A549R cells. Bars represent 20 μm. (b) and (c) Cellular uptake of polyplex micelles against A549R cells after 3 h incubation examined by flow cytometry. A: **PM3**, pH 7.4; B: **PM3**, pH 6.8; C: **PM4**, pH 7.4; D: **PM4**, pH 6.8.

To verify design concept of the proposed polyplex micelle for facilitating cellular uptake of platinum drug into cisplatin-resistant cells A549R, the intracellular Pt content was determined by quantification of Pt concentration in the cell lysis solution from a ICP-MS assay. Cisplatin or polyplex micelles containing same concentrations of Pt (0.4 μM) were incubated with a same amount of cells (1×10^5 cells). As shown in Fig. S4, A549R cells present very low uptake amount of cisplatin, affirmed high cisplatin drug resistant properties of A549R cells. On the contrary, both polyplex micelles, **PM1** and **PM2**, showed remarkable jump in the cellular uptake efficiency at both pH 7.4 and 6.8, this jump probably ascribed to a different internalization mechanism in contrast to cisplatin molecule. Notably, **PM1** at pH 6.8 showed a pronounced increase in cellular uptake of platinum content with 1.91 ± 0.09 ng/mg protein as compared to that of at pH 7.4 with 0.91 ± 0.02 ng/mg protein. On the other hand, **PM2** mediated similar level of intracellular platinum contents at pH 7.4 and 6.8,

Journal of Materials Chemistry B Accepted Manuscript

and this value was comparable to that of **PM1** at pH 7.4.

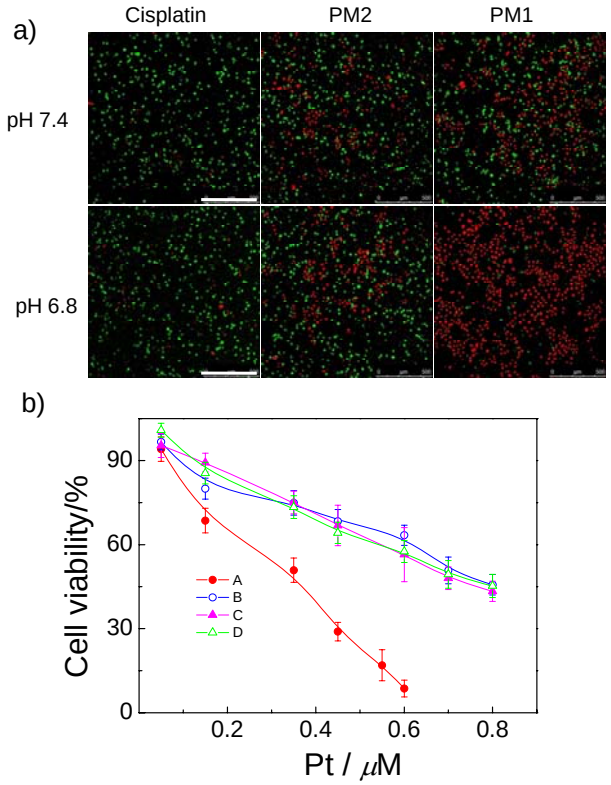

Fig. 5 (a) CLSM images of calcein AM (green, live cells) and PI (red, dead cells) costained A549R cells after treatment with the polyplex micelles (**PM1** and **PM2**) at pH 7.4 or pH 6.8. The Pt concentration was fixed at 0.6 μM. Scale bars represent 500 μm. (b) The cytotoxicity of varying polyplex micelles against A549R cells (mean ± SEM, n = 4). A: **PM1**, pH 6.8; B: **PM1**, pH 7.4; C: **PM2**, pH 6.8; D: **PM2**, pH 7.4.

Cytotoxicity

Firstly, we investigated in vitro cancer cells (A549R) ablation after treatment of polyplex micelles at Pt concentration of 0.6 μM. After incubation of cells with **PM1** and **PM2** for 3 h at pH 6.8 or pH 7.4 followed by further 24 h incubation, the cells were subsequently stained with both calcein AM (green, live cells) and PI (red, dead cells).[51] Fig. 5a shows that florescent images of live cells and dead cells captured with a CLSM. Apparently, the cisplatin-resistant cells were not killed by cisplatin at the concentration of 0.6 μM both at pH 7.4 and pH 6.8. In contrast, for **PM1** at pH 7.4 and **PM2** at both pH 7.4 and pH 6.8, almost half of the cells were killed. Notably, **PM1** at pH 6.8 showed much larger red zone reflecting much greater cancer cells killing ability due to the dissociation of **PM1** and higher cellular internalization as compared with **PM1** at pH 7.4 and **PM2** at both pH 7.4 and pH 6.8.

Moreover, Pt concentration-dependent cytotoxicity of **PM1** and **PM2** were evaluated in detail. The in vitro cytotoxicity of free cisplatin, **PM1**, and **PM2** against A549 and A549R cells was evaluated by a MTT assay. The cells were incubated for 3 h at pH 7.4 and 6.8 in presence of varying samples for cellular uptake, followed by further 48 h incubation to allow the affected cells to undergo apoptosis. It should be noted that the block copolymers and PAMAM dendrimers have much lower cytotoxicity to the culture cells at the current concentrations as compared with the anti-cancer drugs.[35,36] Thus, cytotoxicity was mainly induced by the anti-cancer drugs. Firstly, the cytotoxicity of anticancer drug cisplatin to A549 and A549R cells were evaluated, and the half-maximal inhibitory concentrations (IC50) of them were determined to be 5.59 and 29.09, respectively (Table 1). This result approved the high cisplatin drug resistance of A549R cells. The underlying mechanism of drug resistance of cisplatin to the cancer cells may be attributed to low drug uptake resulting from the low expression of copper transport protein (Ctr1) and deactivation by the high concentration of metallothionein (MT) and small peptide glutathione (GSH).[20] As shown in Fig. 5b, **PM1** and **PM2** at pH 7.4 showed comparable cytotoxicity to A549R cells since the alternative endocytosis pathway of Pt(IV) prodrug loading nanoparticles was identified so as to overcome the drug resistance of cisplatin to the cancer cells.[19,20] and the IC50 values were much lower than that of cisplatin. Moreover, **PM1** showed considerably higher cytotoxicity at pH 6.8. The IC50 of the platinum in **PM1** at pH 6.8 was 2.2-folded lower than that at pH 7.4 due to higher cellular internalization activity at pH 6.8 (Table 1). The internalization of G3-PAMAM was involved both caveolae-dependent endocytosis and macropinocytosis pathways,[47] leading to high cellular uptake and cytotoxicity against A549R cells. On the other hand, **PM2** preserved the complex structure at both pH 6.8 and pH 7.4, and showed higher IC50 values as compared with those of **PM1** at pH 6.8.

Table 1 Half-maximal inhibitory concentration (IC50) of cisplatin and varying polyplex micelles against A549 and A549R as determined by MTT assay (Pt concentration/μM).

Cells	Cisplatin	PM1		PM2	
		6.8[b]	7.4[b]	6.8[b]	7.4[b]
A549	5.59	0.31	0.72	/	/
A549R	29.09	0.33	0.73	0.68	0.70
RF[a]	5.20	/	/	/	/

[a] RF: resistant factor; [b] pH values.

Collagen gel diffusion

As demonstrated, **PM1** is able to dissociate under tumoral acidity (pH 6.8) and release G3-PAMAM-Pt(IV) conjugates. In view of small size of G3-PAMAM-Pt(IV) dendrimers, it is reasonable to anticipate deep penetration in the tumor tissue. To verify this hypothesis, we evaluate diffusive transport of **PM3** using a collagen gel to resemble interstitial matrix of a solid tumor, which were obtained by injecting 53 μL collagen gel in a capillary tube at the concentration of 7.54 mg/mL.[21,22] 3 μL of **PM3** after 1 h preincubation at 7.4 or 6.8 was placed in contact with the gel and incubated for 4 h. Notably, pH values of collagen gels were firstly measured after adding the micelles onto collagen gels due to pH-sensitivity of collagen gels,[52,53] which showed that the pH values remained almost unchanged for both of the two samples probably owing to the buffering capacity of collagen gel solutions and addition of relatively small amount of micelle solution. Thus, the physical structures of the collagen gels were thought to maintain constant upon addition of polyplex micelle solutions. CLSM was used to gain insight on infiltration activities

Journal of Materials Chemistry B Accepted Manuscript

of each sample into the collagen gel (Fig. 6). **PM3** incubated at pH 7.4 exhibited very limited penetration. On the contrary, the G3-PAMAM-FITC nanoparticles at pH 6.8 inspired a 2 millimeters depth penetration into the gel within 4 h as a result of the dissociation of **PM3**.

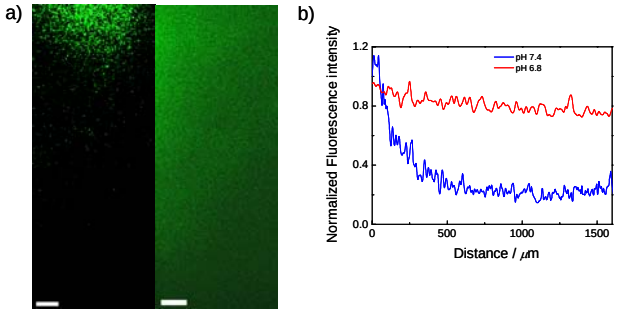

Fig. 6 (a) Penetration profile of **PM3** into the collagen hydrogel at pH 7.4 (left lane) and pH 6.8 (right lane). Scale bars in the images represent 125 μm. (b) Normalized fluorescent intensity of **PM3** in collagen hydrogels at pH 7.4 and pH 6.8.

Penetration in MCTS

Three-dimensional (3D) in vitro tumor model, MCTS with diameter > 200 μm, was employed as a resembled model to study the efficacy of our proposed system for tumor penetration and anti-tumor efficacy. A549R cells were used to formulate the 3D tissue model MCTs. Fig. 7a shows the morphologies of A549R MCTS captured by optical microscope. The MCTS exhibited as homogeneous bulk characterized with 300 μm symmetrical sphere in terms of diameter. To investigate the penetration behaviors of **PM3** in MCTS, the A549R MCTS were pre-incubated with the polyplex micelles at culture medium of pH 7.4 or pH 6.8. CLSM was used to investigate the penetration of G3-PAMAM-FITC by the equatorial slice images of A549R spheroids, which were frequently utilized to study tissue penetration of anti-cancer drug delivery nanoparticles.[27,54] Fig. 7b showed typical CLSM images of A549R MCTS incubated with **PM3** at pH 7.4 or 6.8 for 3 h, 8 h and 24 h, respectively. It is apparent that the fluorescence of G3-PAMAM-FITC was limited at the periphery of MCTS after the first 3 h incubation at pH 7.4. As opposed to pH 7.4, abundant fluorescence was localized inside the MCTS at pH 6.8. After 8 h incubation at pH 6.8, G3-PAMAM-FITC dendrimers distributed uniformly within the entire MCTS indicating that G3-PAMAM-FITC dendrimers penetrated into the center of the MCTS. The fluorescence at pH 7.4 can merely reach 50 μm from the periphery even with 8 h incubation. Quantitatively, markedly stronger fluorescence intensities were found to be inside the MCTS after 3 h, 8 h, and 24 h incubation at pH 6.8 in stark contrast with those at pH 7.4 (Fig. 7c). These results approved that G3-PAMAM-FITC dendrimers released from **PM3** at pH 6.8 facilitated penetration into tumor tissue by virtue of small size.

MCTS growth inhibition

To evaluate growth inhibition of varying drug formulations to the cisplatin-resistant human lung cancer A549R MCTS, MCTS were incubated with cisplatin or **PM1** with an entire platinum concentration of 0.4 μM at pH 7.4 and pH 6.8 for 24 h. The MCTS were allowed to culture in fresh medium (medium exchange every 24 h) for growth at pH 7.4 for 7 days. Fig. 8a lists the representative optical images of MCTS after treatment with diverse drug formulations. Notably, no significant growth inhibition was observed for the MCTS treated with cisplatin. The diameter and MCTS increased over time from ~ 250 μm to ~ 300 μm due to the cisplatin drug resistance of MCTS from A549R cancer cell lines (Fig. 8b). This result suggests drug resistance required to be resolved to attain therapeutic potency. On the other hand, **PM1** at pH 7.4 afforded a distinct growth inhibition on the growth of the MCTS as compared to cisplatin. The average diameter of MCTS dropped from ~ 300 μm to ~ 220 μm with seven-day post culture. To our interests, the treatment with **PM1** at pH 6.8 exerted a potent inhibition on the growth of MCTS. At 7 day post administration, the diameter of MCTS decreased from ~ 300 μm to less than 100 μm, which is believed to be due to deep penetration and higher cellular uptake of G3-PAMAM-Pt(IV) as a result of polyplex micelle dissociation at mild acidic pH 6.8.

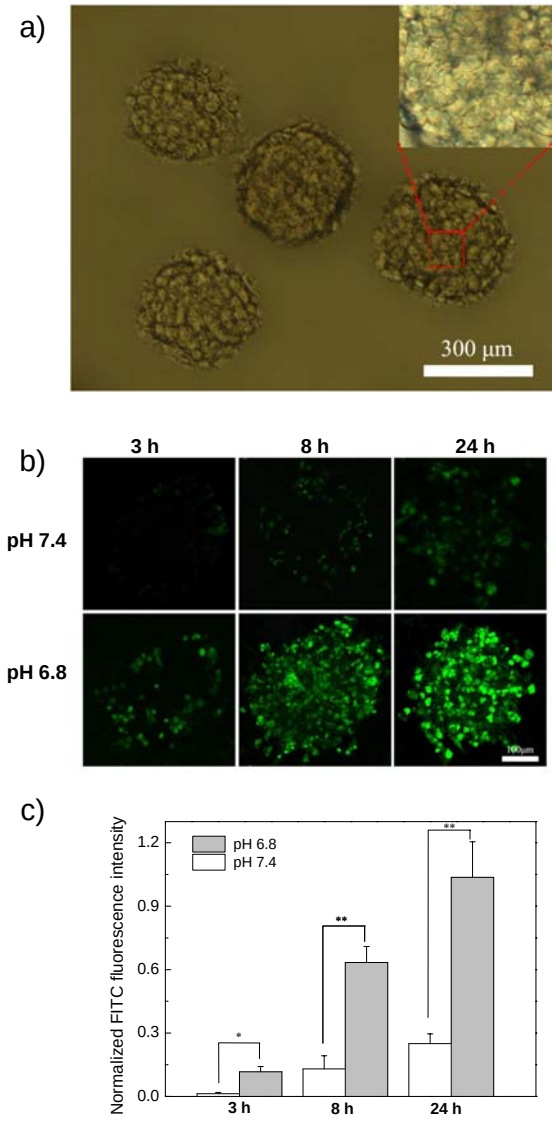

Fig. 7 (a) The morphologies of A549R MCTS observed by optical microscope. (b) Representative equatorial slice images of A549R MCTS incubated with **PM3** at pH 7.4 or 6.8 for 3 h, 8 h and 24 h, respectively. (c) Normalized FITC fluorescence intensity in A549R MCTS (mean ± SEM, n = 10; student't test, $*P < 0.05$, $**P < 0.01$).

Journal of Materials Chemistry B Accepted Manuscript

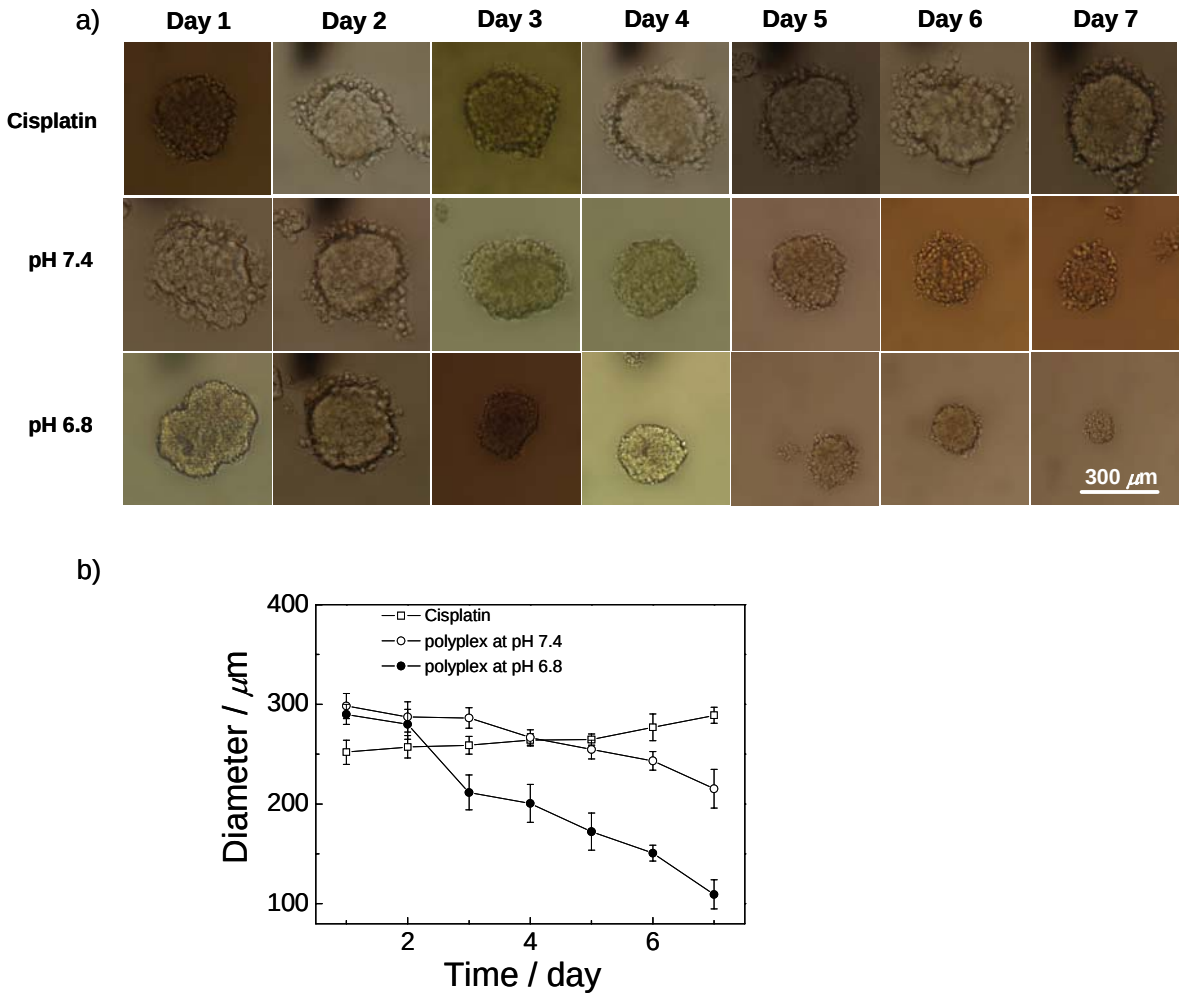

Fig. 8 Growth inhibition assay in treatment of A549R MCTS. (a) Representative images of MCTS treated with cisplatin and **PM1** at pH 7.4 or pH 6.8 with platinum concentration of 0.4 μM. (b) Growth of A549R MCTS after treatments with differing samples (mean ± SEM, n = 10).

Conclusions

We have programmed dual stimulus-responsive polyplex micelles pertaining to tumoral acidity and intracellular reductive environment and achieved tempting two-step drug delivery behavior for deep and massive drug delivery to the tumor cells. This system was constructed from complexation between mild acidic pH-responsive charge-conversional block copolymers, PEG-PAsp(EDA-DM) and PAMAM-Pt(IV) prodrugs. According to optimization for the chemical structures of each component, such as the block copolymer length and PAMAM dendrimer generation, polyplex micelles with suitable size and low size distribution were obtained. Furthermore, the tumoral pH (~ pH 6.8) responsive polyplex dissociation and reductive environment-responsive drug release were demonstrated. The collagen gel diffusion and MCTS penetration experiments verified efficient penetration into the dense tumor tissue as a result of dissociation of polyplex micelles. Moreover, IC50 values of **PM1** at pH 6.8 were observed to give a pronounced 88 times than cisplatin drug against drug resistant A549R cells. The efficient drug penetration together with elevated drug potency contributed to a significant growth inhibition of A549R MCTS. The obtained results approved this smart polyplex micelle drug delivery system manage to overcome the barriers of tumor tissue penetration and drug resistance. Our proof-of-concept design provided a novel design of anticancer drug delivery system, capable of overcoming the pre-defined biological barriers via unique multistage delivery responsive to the specific biological microenvironments. It should be pointed out that the stability of the polyplex micelles in blood circulation could be facilely improved for *in vivo* application by introduction of hydrophobic segments or cross-linking points.[55,56] Further work towards this aspect is currently underway.

Acknowledgements

The financial support from National Natural Scientific Foundation of China (NNSFC) Project (51273188, 81201176), A Foundation for the Author of National Excellent Doctoral Dissertation of PR China (FANEDD) (2012240), the Specialized Research Fund for the Doctoral Program of Higher Education (SRFDP) (20123402120022), Anhui Provincial Natural Science Foundation (APNSF) (1208085QB21) is gratefully acknowledged.

Notes and references

Journal of Materials Chemistry B Accepted Manuscript

[a] CAS Key Laboratory of Soft Matter Chemistry, Department of Polymer Science and Engineering, University of Science and Technology of China, Hefei, Anhui 230026, China Tel:+81-551-63603670; E-mail: gezs@ustc.edu.cn
[b] Department of Materials Engineering, Graduate School of Engineering, The University of Tokyo, 7-3-1 Hongo, Bunkyo-ku, Tokyo 113-8656, Japan. E-mail: chenqixian1985@gmail.com
[c] CAS Key Laboratory of Soft Matter Chemistry, Department of Chemistry, University of Science and Technology of China, Hefei, Anhui 230026, China
[d] Department of Chemistry, Quaid-I-Azam University, Islamabad 45320, Pakistan

† Electronic Supplementary Information (ESI) available: Scheme S1, Table S1, Fig.S1-S4. See DOI: 10.1039/b000000x/

1 N. Kamaly, Z. Y. Xiao, P. M. Valencia, A. F. Radovic-Moreno and O. C. Farokhzad, *Chem. Soc. Rev.*, 2012, **41**, 2971-3010.
2 J. W. Nichols and Y. H. Bae, *Nano Today*, 2012, **7**, 606-618.
3 H. Cabral, N. Nishiyama and K. Kataoka, *Acc. Chem. Res.*, 2011, **44**, 999-1008.
4 D. Peer, J. M. Karp, S. Hong, O. C. FaroKHzad, R. Margalit and R. Langer, *Nat. Nanotechnol.*, 2007, **2**, 751-760.
5 N. Nishiyama, Y. Morimoto, W. D. Jang and K. Kataoka, *Adv. Drug Deliv. Rev.*, 2009, **61**, 327-338.
6 R. K. Jain and T. Stylianopoulos, *Nat Rev Clin Oncol*, 2010, **7**, 653-664.
7 D. E. Owens and N. A. Peppas, *Int. J. Pharm.*, 2006, **307**, 93-102.
8 A. Vonarbourg, C. Passirani, P. Saulnier and J. P. Benoit, *Biomaterials*, 2006, **27**, 4356-4373.
9 A. I. Minchinton and I. F. Tannock, *Nat. Rev. Cancer*, 2006, **6**, 583-592.
10 F. Marcucci and A. Corti, *Adv. Drug Deliv. Rev.*, 2012, **64**, 53-68.
11 T. Lammers, F. Kiessling, W. E. Hennink and G. Storm, *J. Control. Release*, 2012, **161**, 175-187.
12 W. J. Gradishar, S. Tjulandin, N. Davidson, H. Shaw, N. Desai, P. Bhar, M. Hawkins and J. O'Shaughnessy, *J. Clin. Oncol.*, 2005, **23**, 7794-7803.
13 M. E. R. O'Brien, N. Wigler, M. Inbar, R. Rosso, E. Grischke, A. Santoro, R. Catane, D. G. Kieback, P. Tomczak, S. P. Ackland, F. Orlandi, L. Mellars, L. Alland, C. Tendler and C. B. C. S. Grp, *Ann Oncol*, 2004, **15**, 440-449.
14 H. Cabral, Y. Matsumoto, K. Mizuno, Q. Chen, M. Murakami, M. Kimura, Y. Terada, M. R. Kano, K. Miyazono, M. Uesaka, N. Nishiyama and K. Kataoka, *Nat. Nanotechnol.*, 2011, **6**, 815-823.
15 V. P. Chauhan, T. Stylianopoulos, J. D. Martin, Z. Popovic, O. Chen, W. S. Kamoun, M. G. Bawendi, D. Fukumura and R. K. Jain, *Nat. Nanotechnol.*, 2012, **7**, 383-388.
16 S. D. Perrault, C. Walkey, T. Jennings, H. C. Fischer and W. C. W. Chan, *Nano Lett.*, 2009, **9**, 1909-1915.
17 Y. Boucher, L. T. Baxter and R. K. Jain, *Cancer Res.*, 1990, **50**, 4478-4484.
18 M. E. Davis, Z. Chen and D. M. Shin, *Nat. Rev. Drug Discov.*, 2008, **7**, 771-782.
19 C. M. J. Hu and L. F. Zhang, *Biochem. Pharmacol.*, 2012, **83**, 1104-1111.
20 Y. Z. Min, C. Q. Mao, S. M. Chen, G. L. Ma, J. Wang and Y. Z. Liu, *Angew. Chem., Int. Ed.*, 2012, **51**, 6742-6747.
21 R. Tong, H. D. Hemmati, R. Langer and D. S. Kohane, *J. Am. Chem. Soc.*, 2012, **134**, 8848-8855.
22 C. Wong, T. Stylianopoulos, J. A. Cui, J. Martin, V. P. Chauhan, W. Jiang, Z. Popovic, R. K. Jain, M. G. Bawendi and D. Fukumura, *Proc. Natl. Acad. Sci. U. S. A.*, 2011, **108**, 2426-2431.
23 Z. Ge and S. Liu, *Chem. Soc. Rev.*, 2013, **42**, 7289-7325.
24 B. Godin, E. Tasciotti, X. W. Liu, R. E. Serda and M. Ferrari, *Acc. Chem. Res.*, 2011, **44**, 979-989.
25 Y. Lee, S. Fukushima, Y. Bae, S. Hiki, T. Ishii and K. Kataoka, *J. Am. Chem. Soc.*, 2007, **129**, 5362-5363.
26 S. Dhar, W. L. Daniel, D. A. Giljohann, C. A. Mirkin and S. J. Lippard, *J. Am. Chem. Soc.*, 2009, **131**, 14652-14653.
27 X. Wang, X. Zhen, J. Wang, J. L. Zhang, W. Wu and X. Q. Jiang, *Biomaterials*, 2013, **34**, 4667-4679.
28 Y. Lee, T. Ishii, H. Cabral, H. J. Kim, J. H. Seo, N. Nishiyama, H. Oshima, K. Osada and K. Kataoka, *Angew. Chem., Int. Ed.*, 2009, **48**, 5309-5312.
29 Z. X. Zhou, Y. Q. Shen, J. B. Tang, M. H. Fan, E. A. Van Kirk, W. J. Murdoch and M. Radosz, *Adv. Funct. Mater.*, 2009, **19**, 3580-3589.
30 J. Z. Du, X. J. Du, C. Q. Mao and J. Wang, *J. Am. Chem. Soc.*, 2011, **133**, 17560-17563.
31 X. Z. Yang, J. Z. Du, S. Dou, C. Q. Mao, H. Y. Long and J. Wang, *Acs Nano*, 2012, **6**, 771-781.
32 S. Sunoqrot, J. W. Bae, R. M. Pearson, K. Shyu, Y. Liu, D. H. Kim and S. Hong, *Biomacromolecules*, 2012, **13**, 1223-1230.
33 D. A. Tomalia, L. A. Reyna and S. Svenson, *Biochem. Soc. Trans.*, 2007, **35**, 61-67.
34 Y. Y. Cheng, L. B. Zhao, Y. W. Li and T. W. Xu, *Chem. Soc. Rev.*, 2011, **40**, 2673-2703.
35 X. Wang, X. Cai, J. Hu, N. Shao, F. Wang, Q. Zhang, J. Xiao and Y. Cheng, *J. Am. Chem. Soc.*, 2013, **135**, 9805-9810.
36 S. J. Zhu, L. L. Qian, M. H. Hong, L. H. Zhang, Y. Y. Pei and Y. Y. Jiang, *Adv. Mater.*, 2011, **23**, 84-89.
37 K. Y. Huang, H. L. Ma, J. Liu, S. D. Huo, A. Kumar, T. Wei, X. Zhang, S. B. Jin, Y. L. Gan, P. C. Wang, S. T. He, X. N. Zhang and X. J. Liang, *Acs Nano*, 2012, **6**, 4483-4493.
38 B. Kim, G. Han, B. J. Toley, C. K. Kim, V. M. Rotello and N. S. Forbes, *Nat. Nanotechnol.*, 2010, **5**, 465-472.
39 S. P. Hong, A. U. Bielinska, A. Mecke, B. Keszler, J. L. Beals, X. Y. Shi, L. Balogh, B. G. Orr, J. R. Baker and M. M. B. Holl, *Bioconjugate Chem.*, 2004, **15**, 774-782.
40 Y. Li, H. He, X. R. Jia, W. L. Lu, J. N. Lou and Y. Wei, *Biomaterials*, 2012, **33**, 3899-3908.
41 C. Dufes, I. F. Uchegbu and A. G. Schatzlein, *Adv. Drug Deliv. Rev.*, 2005, **57**, 2177-2202.
42 H. H. Xiao, R. G. Qi, S. Liu, X. L. Hu, T. C. Duan, Y. H. Zheng, Y. B. Huang and X. B. Jing, *Biomaterials*, 2011, **32**, 7732-7739.
43 X. Y. Wang and Z. J. Guo, *Chem. Soc. Rev.*, 2013, **42**, 202-224.
44 N. Kolishetti, S. Dhar, P. M. Valencia, L. Q. Lin, R. Karnik, S. J. Lippard, R. Langer and O. C. Farokhzad, *Proc. Natl. Acad. Sci. U. S. A.*, 2010, **107**, 17939-17944.
45 R. P. Feazell, N. Nakayama-Ratchford, H. Dai and S. J. Lippard, *J. Am. Chem. Soc.*, 2007, **129**, 8438-8439.
46 K. M. Kitchens, A. B. Foraker, R. B. Kolhatkar, P. W. Swaan and H. Ghandehari, *Pharm. Res.*, 2007, **24**, 2138-2145.
47 A. Saovapakhiran, A. D'Emanuele, D. Attwood and J. Penny, *Bioconjugate Chem.*, 2009, **20**, 693-701.
48 V. A. Sethuraman, K. Na and Y. H. Bae, *Biomacromolecules*, 2006, **7**, 64-70.
49 H. Hatakeyama, H. Akita, E. Ito, Y. Hayashi, M. Oishi, Y. Nagasaki, R. Danev, K. Nagayama, N. Kaji, H. Kikuchi, Y. Baba and H. Harashima, *Biomaterials*, 2011, **32**, 4306-4316.
50 J. Li, Z. Ge and S. Liu, *Chem. Commun.*, 2013, **49**, 6974-6976.
51 V. Voliani, G. Signore, O. Vittorio, P. Faraci, S. Luin, J. Perez-Prieto and F. Beltram, *J. Mater. Chem. B*, 2013, **1**, 4225-4230.
52 T. Hayashi and Y. Nagai, *J. Biochem.*, 1973, **73**, 999-1006.
53 J. Rosenblatt, B. Devereux and D. G. Wallace, *Biomaterials*, 1994, **15**, 985-995.
54 K. Kostarelos, D. Emfietzoglou, A. Papakostas, W. H. Yang, A. Ballangrud and G. Sgouros, *Int. J. Cancer*, 2004, **112**, 713-721.
55 S. Herlambang, M. Kumagai, T. Nomoto, S. Horie, S. Fukushima, M. Oba, K. Miyazaki, Y. Morimoto, N. Nishiyama and K. Kataoka, *J. Control. Release*, 2011, **155**, 449-457.
56 M. Oba, K. Miyata, K. Osada, R. J. Christie, M. Sanjoh, W. D. Li, S. Fukushima, T. Ishii, M. R. Kano, N. Nishiyama, H. Koyama and K. Kataoka, *Biomaterials*, 2011, **32**, 652-663.

Journal of Materials Chemistry B Accepted Manuscript